Synthesis and Characterization of Nylon 1012/Clay Nanocomposite

ZENGGANG WU,[1] CHIXING ZHOU,[1,2] RONGRONG QI,[1] HONGBIN ZHANG[1]

[1] College of Chemistry and Chemical Technology, Shanghai Jiaotong University, Shanghai 200240, People's Republic of China

[2] Department of Chemistry, Jilin University, State Key Laboratory of Polymer Physics and Chemistry, Changchun, People's Republic of China

Received 21 February 2001; accepted 8 July 2001

ABSTRACT: A nylon 1012/clay nanocomposite was prepared by melt polycondensation polymerization of diamine and diacid in the presence of organoclay. The nylon 1012 and nanocomposite were characterized by Fourier transform IR spectroscopy with attenuated total reflection, and a shift of the Si—O—Si band toward a lower wavenumber was found as the result of the strong interaction of nylon 1012 with the organoclay. The X-ray diffraction analysis and transmission electron microscopy observation showed that the clay minerals were exfoliated. Clay platelets increased the crystallization rate but decreased the crystallinity. Differential scanning calorimetry and dynamic mechanical thermal analysis measurements showed that the glass-transition temperature of the nylon 1012/clay nanocomposite decreased to some degree as compared to nylon 1012 because of the combined effect of confinement and the reduction of the physical crosslink density. The mechanical properties of the nanocomposite such as the tensile strength and tensile modulus are higher than those of nylon 1012, and the water absorption is reduced because of the improvement in the barrier property of the nanocomposite. © 2002 John Wiley & Sons, Inc. J Appl Polym Sci 83: 2403–2410, 2002

Key words: nanocomposite; nylon 1012; melt polycondensation polymerization; clay; exfoliation

INTRODUCTION

Polymer-layered silicate (PLS) nanocomposites are a combination of nanometer-sized clay platelets with a polymer matrix. These nanocomposites usually exhibit superior properties to those of the pristine polymer and conventional inorganic particle filled composite materials because of the synergistic effects from the two constituting components and the strong interaction between the high specific area nanoclay and the polymer. The first commercialized PLS nanocomposite is a nylon 6/clay hybrid in which the long molecular chains were tethered to the clay platelet surface.[1] This confinement of the chains and strong interaction between the clay and polymer render the nanocomposite with unusual properties, such as high tensile strength, high tensile modulus, high heat distortion temperature, and good gas barrier property. Compared with conventional composite materials, the nanocomposites also possess the advantage of low loading (usually $< 5\%$), which leads to little sacrifice of impact properties.[2]

Correspondence to: C. Zhou (cxzhou@mail.sjtu.edu.cn).

Contract grant sponsor: National Natural Science Foundation of China.

Journal of Applied Polymer Science, Vol. 83, 2403–2410 (2002)

DOI 10.1002/app.10198

Nylon 1012 is a recently industrialized engineering plastic with a lower melting temperature, slightly lower density, excellent impact behavior, lower dielectric constant, and lower water affinity than other common short chain nylons such as nylon 6 and nylon 66.[3] In some special applications, nylon 1012 has the advantages over some polyolefins of its higher melting temperature and better bonding to adhesives and paint. Therefore, it is of great importance to study this nylon 1012/clay nanocomposite.

The first commercially valuable nylon 6/clay hybrid[1] was synthesized by *in situ* ring-opening polymerization of ϵ-caprolactam with protonated 12-aminolauric acid exchanged clay, and a similar method was successfully applied to the preparation of a nylon 12/clay nanocomposite.[4] Two recent studies[5,6] prepared the nylon 6/clay hybrid by an environmentally benign melt intercalation on a lab scale. Recently RTP Company announced that they produced the first commercially available product that incorporates organoclay hybrids into nylon via a compounding process.[7] However, few published documents were focused on the preparation of polyamide from diamine and diacid.[8,9] The purpose of this article is to investigate the preparation of a kind of copolyamide nanocomposite nylon 1012/clay nanocomposite by melt polycondensation polymerization of diamine and diacid. The morphological, thermal, and mechanical behaviors of the nanocomposite were also studied using Fourier transform IR spectroscopy with attenuated total reflection (FTIR-ATR), X-ray diffraction (XRD), transmission electron microscopy (TEM), dynamic mechanical thermal analysis (DMTA), and differential scanning calorimetry (DSC).

EXPERIMENTAL

Materials

The clay and organoclay were kindly supplied by Huate Co. Ltd. The cation exchange capacity was about 85–110 meq/100 g of montmorillonite. 1,10-Decanedicarboxylic acid and 1,10-diaminodecane were purchased from Aldrich and used as received.

Sample Preparation

Synthesis of Nylon 1012

The synthesis procedure was according to a reference method.[8] 1,10-Decanedicarboxylic acid (4.60 g, 0.02 mol) was dissolved in absolute alcohol (50 mL) at 50°C, and a solution of 1,10-diaminodecane (3.61 g, 0.021 mol) in absolute alcohol (30 mL) was added under vigorous stirring. A diaminodecane-decanedicarboxylic acid salt immediately precipitated. The mixture was stirred for another 30 min at 50°C and then cooled to room temperature. A white product was collected by filtration. The salt was recrystallized from a mixture of alcohol (130 mL) and water (40 mL) and was obtained as a white powder (6.98 g, 85%).

Diaminodecane-decanedicarboxylic acid salt (6.03 g, 0.015 mol) and a slight excess of diaminodecane (0.025 g, 0.15 mmol) were added to a U-shaped glass tube equipped with a nitrogen inlet and an outlet. The glass tube was purged with nitrogen before the reaction. This process was repeated at least 3 times. The glass tube was immersed in an oil bath and the temperature was quickly raised to 200°C to start the reaction. After maintaining the autoclave for 2 h at 200°C, the temperature was increased to 215°C and held for 1.5 h under these conditions. The glass tube was flushed with nitrogen each time to bring out the water produced in polycondensation. In the last step a vacuum (< 0.1 atm) was established to get rid of the water and residual monomer, the temperature was increased to 225°C, and the reaction was continued for another 2 h. The glass tube was then cooled to room temperature. The resulting nylon 1012 was obtained as a white solid (5.12 g, 85%) and was pulverized in a freezing mill.

Synthesis of Nylon 1012/Clay Nanocomposite

The organoclay (0.25 g) was dispersed in absolute alcohol (50 mL) and sonicated for 10 min. The dispersion was added to 1,10-diaminodecane (3.61 g, 0.021 mol) in absolute alcohol (30 mL) and sonicated for another 30 min to attain a mixture. Then the mixture was added to the absolute alcohol solution of 1,10-decanedicarboxylic acid (4.60 g, 0.02 mol) to obtain the diaminodecane-decanedicarboxylic acid salt. The following procedure was similar to the synthesis of nylon 1012 as mentioned above.

FTIR-ATR Characterization

The sample film with about 0.5-mm thickness was molded at 10.0 MPa and 200°C for a few minutes and then quenched to room temperature. FTIR-ATR was performed with a Bruker FTIR instrument with ATR accessories. Blank scan-

ning was performed before measurements to eliminate the influence of water vapor and CO_2 in the air.

XRD Analysis and TEM Observation

The XRD analysis was conducted using a Philips PW1710 X-ray diffractometer. The X-ray beam was nickel-filtered CuKα radiation (λ = 1.54060 Å), and data were collected from 1.5 to 30°C (2θ) at a rate of 1.5°C/min. The dispersion of clay lamellae was observed using a JEM-1200EX transmission electron microscope; the ultrathin film (about 500 nm) was cut under cryogenic conditions using a Reichert–Jung Ultracut E microtome. The reason that the ultrathin film is not thinner than 500 nm is to reduce the shrinkage of the film when exposed to the electron beam during observation.

DSC Measurement

Isothermal crystallization and subsequent melting were carried out using a Perkin–Elmer Pyris-1 differential scanning calorimeter with the temperature calibrated with indium. All DSC measurements were performed under nitrogen purge, and samples of about 4–5 mg were cut from the film mentioned above. Isothermal crystallization from the melt was carried out by heating the sample to 210°C and holding for 15 min to eliminate the residual crystals, cooling to 167°C at a rate of 150°C/min and holding there for 25 min to get a complete crystallization, cooling the sample from 167 to 120°C at 40°C/min, and then heating the sample from 120 to 210°C at 10°C/min to record the melting process.

DMTA Testing

The temperature dependence of the mechanical properties (storage modulus G', loss modulus G'', and tan δ) was examined using a Rheometric Scientific DMTA IV. A frequency sweep temperature ramp test was performed at a frequency (ω) of 6.28 rad/s (=1 Hz) from 25 to 180° at a heating rate of 3°C/min using tensile mode. The specimen was about 10 mm long, 8 mm wide, and 0.15 mm thick.

Mechanical Properties and Water Absorption

The dumbbell-shaped specimens were tested using an Instron 4465 universal testing system with a crosshead speed of 50 mm/min.

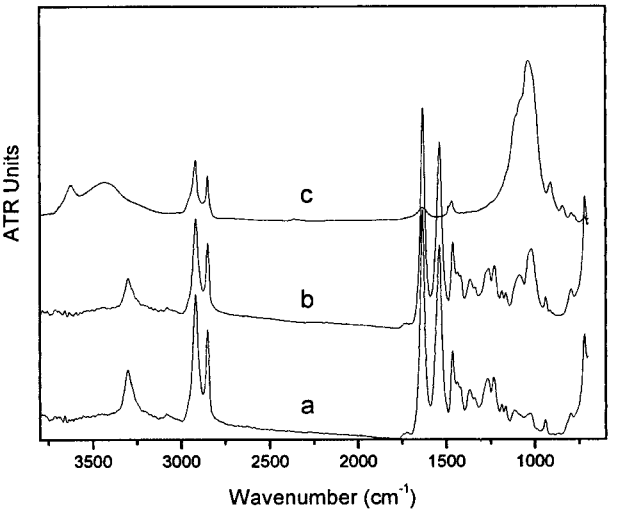

Figure 1 FTIR-ATR spectra for nylon 1012 (spectrum a), nylon 1012/clay nanocomposite (spectrum b), and organoclay (spectrum c).

Samples were dried in a vacuum oven at 80°C overnight before testing and then soaked in deionized water at 25°C for 72 h. The water absorption (w, %) is given by

$$w = \frac{w - w_0}{w_0} \times 100\% \quad (1)$$

where w_0 is the weight before soaking w is the weight after soaking in water.

RESULTS AND DISCUSSION

FTIR-ATR Characterization of Nylon 1012 and Nanocomposite

The FTIR-ATR spectra for the organoclay, nylon 1012, and nylon 1012/clay nanocomposite are shown in Figure 1. The characteristic peaks of polyamide can be found in both the nylon 1012 and nanocomposite spectra [Fig. 1(a,b)]. They are at 1640, 1550, and 3300 cm^{-1} and are attributed to the C═O stretching vibration, combinational absorbance of the N—H bending vibration and C—N stretching vibration, and N—H hydrogen bonding, respectively. In Figure 1(b) two separate bands at 1085 and 1020 cm^{-1} belong to the Si—O and Si—O—Si vibration. However, for the organoclay, there is only one combinational band at 1040 cm^{-1} with a shoulder band at 1085 cm^{-1}. Obviously, the Si—O—Si vibration band for the

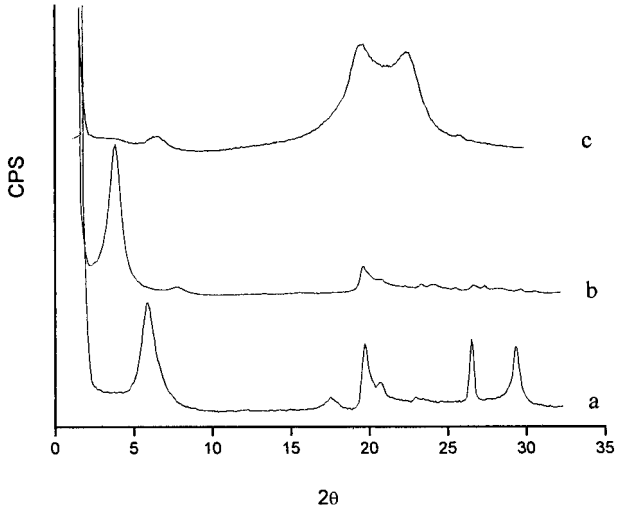

Figure 2 The XRD patterns for clay (spectrum a), organoclay (spectrum b), and nylon 1012/clay nanocomposite (spectrum c).

nylon 1012/clay nanocomposite shifts toward a lower wavenumber, which indicates a strong interaction between the nylon 1012 and organoclay surface.

Morphology of Nanocomposite

The XRD patterns show the spacing change of the clay gallery (d001) according to the Bragg diffraction equation $\lambda = 2d \sin \theta$. Figure 2 illustrates the characteristic peak of the natural clay mineral [Fig. 2 (a)], organoclay [Fig. 2 (b)], and nylon 1012/clay nanocomposite [Fig. 2 (c)]. After the cation-exchange treatment, a shift of about 10 Å in the first clay peak suggests the swelling of the clay galleries with the incorporation of quaternized ammonium [Fig. 2 (b)]. The absence of the characteristic clay d001 peak in Figure 2(c) indicates the exfoliation of the clay platelets in the nylon 1012 matrix. The TEM photomicrograph (Fig. 3) gives a similar result. Disordered clay platelets are homogeneously distributed in the polymer matrix.

Isothermal Crystallization

The DSC curves of isothermal crystallization for nylon 1012 and nylon 1012/clay nanocomposite are shown in Figure 4. The crystallization exothermic peak of the nylon 1012/clay nanocomposite is narrower than that of nylon 1012, indicating that the nanocomposites have a higher crystallization rate. The crystallization heat of the nanocomposite is smaller than that of the nylon 1012, implying that the clay platelets decrease the crystallinity of nylon 1012. Li et al.[10] studied the isothermal and nonisothermal crystallization of nylon 1012 and found that isothermal crystallization could be well described by the Avrami equation. We introduced the Avrami equation into our system and found that it fitted well, too (Fig. 5). The Avrami equation is

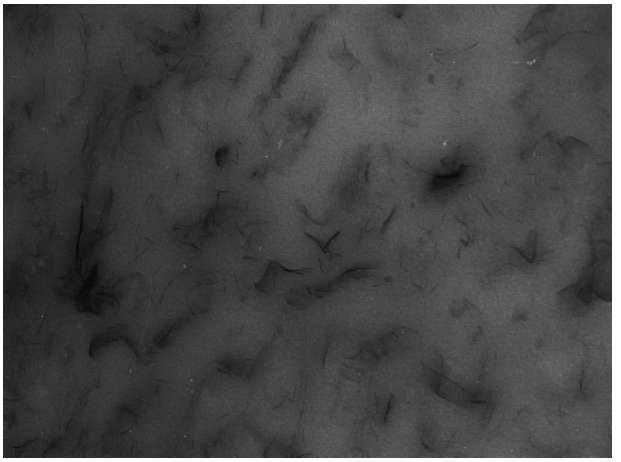

Figure 3 A TEM micrograph of the nylon 1012/clay nanocomposite.

$$Xt = 1 - \exp(-Kt^n)$$

or

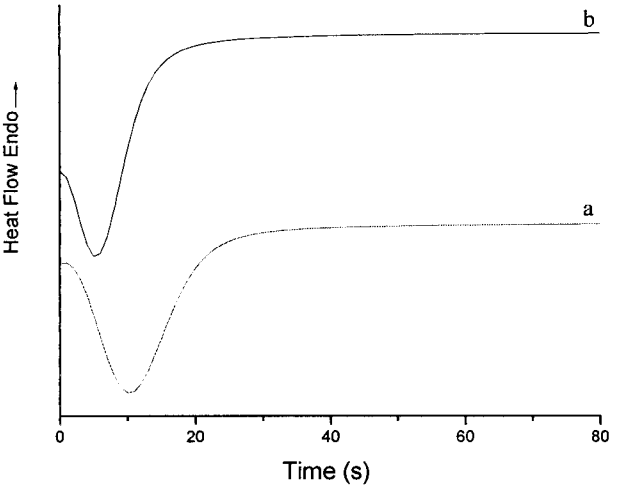

Figure 4 The heat flow versus the time during isothermal crystallization of nylon 1012 (spectrum a) and nylon 1012/clay nanocomposite (spectrum b) by DSC.

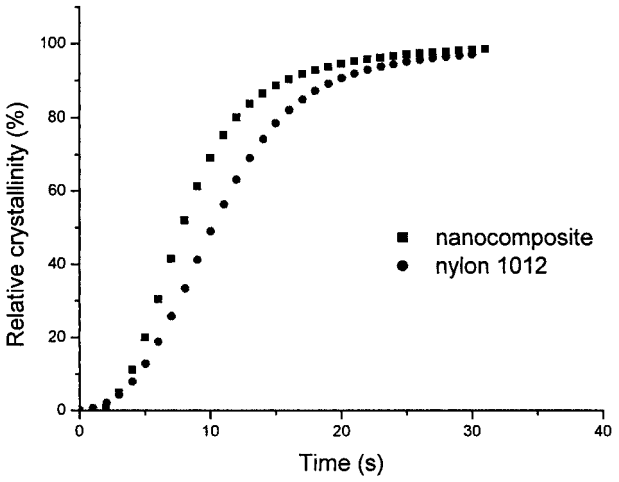

Figure 5 The relative crystallinity versus the time for nylon 1012 and nylon 1012/clay nanocomposite during isothermal crystallization.

$$\log[-\ln(1 - Xt)] = n \log t + \log K \qquad (2)$$

where Xt is the relative crystallinity, K is a constant relative to the nucleation and growth, and n is dependent on the mechanism of nucleation and the dimensions of the crystals. Figures 5 and 6 give a relation of Xt with time in different forms. The $t_{1/2}$ is defined as the time at which the relative crystallinity is 50%, and it can also be derived from the Avrami equation:

$$t_{1/2} = (\ln 2/K)^{1/n} \qquad (3)$$

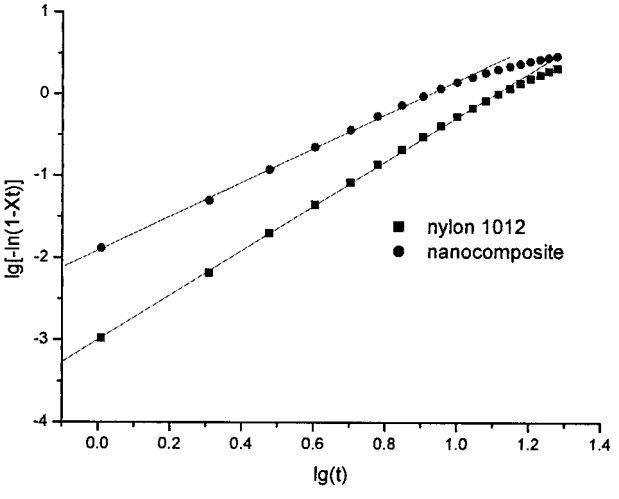

Figure 6 A plot of the $\log[-\ln(1 - Xt)]$ versus $\log t$ for nylon 1012 and nylon 1012/clay nanocomposite.

Table I Parameters of Isothermal Crystallization

	Nylon 1012	Nylon 1012/Clay Nanocomposite
n	2.71	2.07
$\log k$	−2.99	−1.91
$t_{1/2}$ (s)[a]	11.1	7.0
$t_{1/2}$ (s)[b]	10.9	6.8
ΔH (J/g)	−32.07	−21.90

[a] Calculated from the Avrami parameters.
[b] Obtained from Figure 5.

All of these parameters are listed in Table I. The results above show that the crystallization of the nylon 1012/clay nanocomposite can also be described by the Avrami equation.

For nylon 1012 the diamine and diacid both have 10 methylene units, so the chains are more flexible and the segments are more free to adopt a proper arrangement during crystallization than conventional short-chain nylons such as nylon 6 and nylon 66. Usually, crystal formation includes two stages, which are nucleation and crystal growth. Nanometer-sized clay platelets are effective nucleating agents; that is to say, the nanocomposites exhibit heterogeneous nucleation during crystallization. This result is supported by the exponent of the Avrami equation n of the nanocomposite, which is less than that of pure nylon 1012 (Table I). Therefore, the nanocomposite would have a higher crystallization rate than nylon 1012.

To improve the wetting ability with the polymer matrix, the clay is usually modified with large surfactant cations, such as a long chain alkylammonium. After the organotreatment, the nylon and the clay surface have better affinity, which is essential to the dispersion of clay platelets, but this would confine the chains and segmental movement around the platelets. This confinement is also found in other systems. In a nylon 6/clay hybrid[11] the —COOH group of the intercalatant is the initiating point of chain growth during polymerization, so the chains are tethered to the clay surface. It is proved that as much as 60% of the molecular chains[12] are confined by the clay surfaces so that the hybrid has higher modulus and higher strength. Another example for confinement is the poly(ethylene oxide)/clay nanocomposite[13] in which the confinement is so powerful that the glass-transition (T_g) and

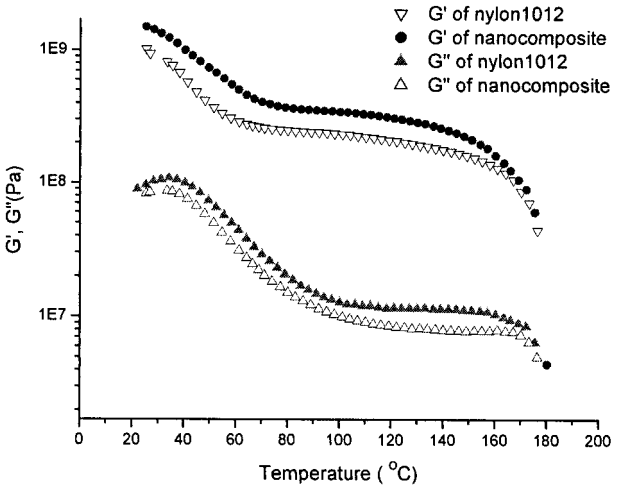

Figure 7 The temperature dependence of G' and G'' for the nylon 1012 and nylon 1012/clay nanocomposite.

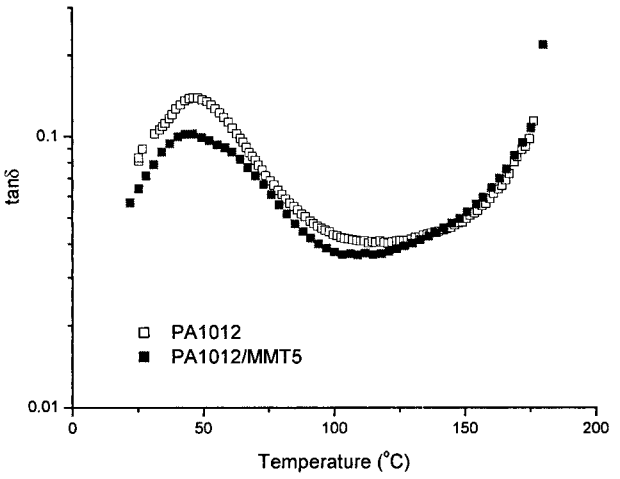

Figure 8 The temperature dependence of tan δ for nylon 1012 and nylon 1012/clay nanocomposite.

melting (T_m) temperatures cannot be detected; in other words, the PEO chains and segments are both "frozen." Therefore, we expect that the confinement to the chains and segments movement will hinder the segmental rearrangement during crystallization and restrict the crystals from the formation of perfect crystals in the nylon 1012/clay nanocomposite. The decrease in the crystallinity is the manifestation of confinement to crystallization in one aspect.

Temperature Dependence of Rheological Properties

Figure 7 gives the temperature dependence of the G' and G''. The G' decreases monotonously with the increasing of the temperature in that temperature range, and there was a sharper decrease near the T_g. The value of G' for the nylon 1012/clay nanocomposite is about 1.5 times that for nylon 1012, while the G'' values for the nanocomposite and nylon 1012 are both comparable at < 90°C. The improvement in the storage modulus may result from the strong interaction between the high surface area of the clay particles and the nylon 1012.

The dependence of the tan δ on the temperature is provided in Figure 8. The temperature at the peak point corresponds to the T_g at which G' decreases faster than G''. Compared to nylon 1012, the peak of the nanocomposite shifts to a lower temperature, which means the T_g is decreased with the addition of clay. A similar result is also detected by DSC measurement (Fig. 9), but the T_g values detected by DSC are higher than those by DMTA. The difference may be due to the different working mechanisms of DSC and DMTA. DSC detects the exothermic or endothermic heat changes with temperature, while DMTA detects the rheological parameters change with temperature. Another reason is the different heating rates in the two measurements: the DSC rate is 20°C/min, and the DMTA rate is 3°C/min.

In many systems the PLS nanocomposite has a higher T_g than the corresponding polymer due to the confinement to the molecular chains. However, for this semicrystalline system, the decrease in crystallinity of the nanocomposite as men-

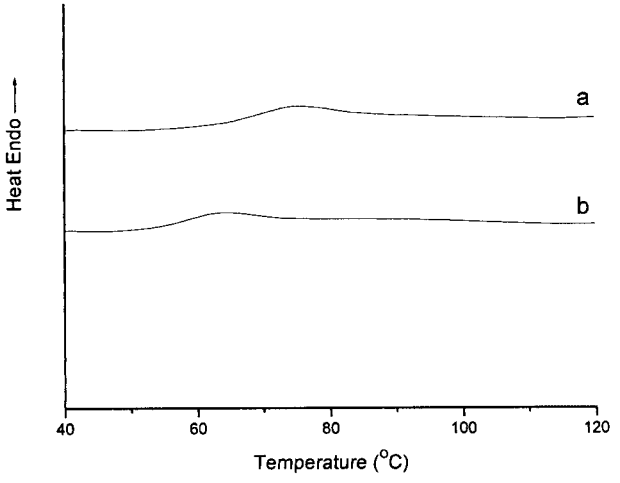

Figure 9 DSC heating curves for nylon 1012 (spectrum a) and nylon 1012/clay nanocomposite (spectrum b).

Table II Mechanical Properties and Water Absorption of Nylon 1012 and Nylon 1012/Clay Nanocomposite

	Tensile Strength (MPa)	Tensile Modulus (GPa)	Elongation (%)	Specific Gravity	Water Absorption (%)
Nylon 1012	31.67 ± 0.5	2.02 ± 0.2	35 ± 5	1.34	3.1
Nylon 1012/clay (1)	33.41 ± 0.5	2.11 ± 0.2	32 ± 5	1.33	2.5
Nylon 1012/clay (3)	38.86 ± 0.5	2.93 ± 0.2	33 ± 5	1.35	2.3
Nylon 1012/clay (5)	43.74 ± 0.6	3.31 ± 0.2	28 ± 4	1.38	1.7

The numbers in parentheses indicate the percentage of clay in the nanocomposite.

tioned above means the reduction in the number of crosslinking points because the crystallite usually acts as the physical crosslinking point. If this outbalances the effect of confinement, a lower T_g will be detected. Shelley et al.[14] found the decrease in T_g of nylon 6/clay nanocomposite and thought that the decrease in the T_g was because of *an increase in the amorphous volume fraction* attributed to the surface–volume ratio of the crystallites, the number of nuclei, and the perfection of the crystal lamellae. Suh et al.[15] also found that a UP/MMT-D nanocomposite had a lower T_g than a corresponding unsaturated polyester because of the low crosslinking density. Another reason for the decrease may be the difference in clay modification. In the nylon 6/clay hybrid the clay is modified with protonated 12-aminolauric acid and the —COOH group of the intercalatant is the initiating point of chain growth during polymerization, so the chains are tethered to the clay surface by chemical bonds. In our system the clay is treated with alkylammonium, which cannot react with the reactant; therefore, nylon 1012 is less confined.

Mechanical Properties and Water Absorption

As shown in Table II, the tensile properties, such as tensile strength and tensile modulus increase by nearly 50% with a little decrease in elongation. The synergistic effect of organoclay and nylon 1012 renders a nanocomposite with pronounced mechanical behaviors, although the weight fraction of clay is $< 5\%$.

As a long-chain nylon, nylon 1012 has a relatively lower hydrophilic amide density; therefore, it would have lower water absorption than other nylons like nylon 6 and nylon 66[16] (saturated water absorption = 9.5 and 8.0%, respectively). In the nylon 1012/clay nanocomposite the surfactant-covered clay platelets form a tortuous path for water transport. This barrier property hinders water from going into the inner part of the nanocomposite.

CONCLUSION

Melt polycondensation polymerization was adopted in the preparation of nylon 1012/clay nanocomposite. The strong interaction at the interface of the nylon 1012 and organoclay was indicated by a shift of the Si—O—Si band toward a lower wavenumber of the FTIR-ATR spectrum. The XRD analysis and TEM observation show that the clay minerals were exfoliated. Clay platelets not only act as nucleating agents and increase the crystallization rate but also confine the movement of molecular chains and segments, resulting in the decrease of crystallinity and T_g. The strong interaction between the organoclay surface and the polymer would endow the nanocomposite with higher tensile strength and higher tensile modulus. The reduction in water absorption is the result of the excellent barrier properties of nanocomposite.

REFERENCES

1. Kojima, Y.; Usuki, A.; Kawasumi, M.; Fukushima, Y.; Kurachi, T.; Kamigaito, O. J Mater Res 1993, 8, 1185.
2. Usuki, A.; Kawasumi, M.; Kojima, Y. J Mater Res 1993, 8, 1174.
3. Melvin, K. Nylon Plastics Handbook; Carl Hanser: New York, 1995.

4. Kim, G.; Lee, D.; Hoffmann, B.; Kressler, J.; Stoppelmann, G. Polymer 2001, 42, 1095.
5. Liu, L.; Qi, Z.; Zhu, X. J Appl Polym Sci 1999, 71, 1133.
6. Cho, J.; Paul, D. Polymer 2001, 42, 1083.
7. John, D. Mechanical Engineering 2001, 123(4), 52.
8. Lan, T.; Connell, G.; Gilmer, J.; Matayabas, J.; Psihogios, V.; Turner, S. International Patent Application WO00/34372, 1998.
9. Lysek, B.; Goettler, L.; Joardar, S.; Middleton, J. International Patent Application WO00/09571, 1998.
10. Li, Y.; Zhu, X.; Yan, D. Polym Sci Eng 2000, 40, 1989.
11. Mathias, L.; Davis, R.; Jarrett, M. Macromolecules 1999, 32, 7958.
12. Nanocor Technical Data G-100, General Information about Nanomers, Nanocor, Arlington Heights, IL, 2000.
13. Vaia, R.; Sauer, B.; Tse, O.; Giannelis, P. J Polym Sci Part B Polym Phys 1997, 35, 59.
14. Suh, D.; Lim, Y.; Park, O. Polymer 2000, 41, 8557.
15. Shi, Z.; Yang, W.; Tang, L. Polyamide Resin Handbook; China Petrochemical Press: Beijing, 1994.
16. Shelley, J. S.; Mather, P. T.; DeVries, K. L. Polymer 2001, 42, 5849.